

**Title Page:**

**Inhibition of phosphodiesterase 10A increases the responsiveness of  
of striatal projection neurons to cortical stimulation**

Sarah Threlfell, Stephen Sammut, Frank S. Menniti, Christopher J. Schmidt, and Anthony R.  
West

Dept. of Neuroscience, Rosalind Franklin University of Medicine and Science, 3333 Green Bay  
Road, North Chicago, IL, 60064, USA (ST, SS, and ARW)

Pfizer Global Research and Development, Eastern Point Road, Groton, CT, 06340, USA (FSM  
and CJS)

**Running title page:**

Running title: Inhibition of phosphodiesterase 10A excites striatal neurons

Corresponding author: Dr. Anthony R. West

Dept. of Neuroscience

Rosalind Franklin University of Medicine and Science, Department of Neuroscience,

3333 Green Bay Road, North Chicago, IL 60064, USA

Tel: 847 578 8658

Fax: 847 578 8515

[Anthony.west@rosalindfranklin.edu](mailto:Anthony.west@rosalindfranklin.edu)

Text pages: 31

Tables: 1

Figures 6

References: 40

Words in abstract: 247

Words in introduction: 690

Words in discussion (not counting references): 1499

**Abbreviations:** aCSF: artificial cerebral spinal fluid; GPe: external globus pallidus; GPi: internal globus pallidus; IT: intratelencephalic; MSNs: medium-sized spiny projection neurons; PDEs: cyclic nucleotide phosphodiesterases; PDE10A: cyclic nucleotide phosphodiesterase 10A; PT: pyramidal tract; SNr+: striatonigral; SNr: substantia nigra pars reticulata; TP-10: 2-{4-[Pyridin-4-yl-1-(2,2,2-trifluoroethyl)-1H-pyrazol-3-yl]-phenoxy}methyl}-quinoline succinic acid

**Section assignment:** Neuropharmacology

## Abstract

The cyclic nucleotide phosphodiesterase 10A (PDE10A) is highly expressed in striatal medium-sized spiny projection neurons (MSNs), apparently playing a critical role in the regulation of both cGMP and cAMP signaling cascades. Genetic disruption or pharmacological inhibition of PDE10A reverses behavioral abnormalities associated with subcortical hyperdopaminergia. Here, we investigate the effect of PDE10A inhibition on the activity of MSNs using single-unit extracellular recordings performed in the dorsal striatum of anesthetized rats. Antidromic stimulation of the substantia nigra pars reticulata was used to identify striatonigral (SNr+) MSNs. Intrastriatal infusion of the selective PDE10A inhibitors papaverine or TP-10 by reverse microdialysis did not affect spontaneous firing, but robustly increased measures of cortically-evoked spike activity in a stimulus intensity-dependent manner. Systemic administration of TP-10 also increased cortically-evoked spike activity in a stimulus intensity- and dose-dependent manner. A robust increase in cortically-evoked activity was apparent in SNr- MSNs (primarily striatopallidal). Interestingly, TP-10 administration did not affect cortically-evoked activity in SNr+ MSNs. However, TP-10 administration increased the incidence of antidromically activated (i.e., SNr+) MSNs. These findings indicate that inhibition of striatal PDE10A activity increases the responsiveness of MSNs to depolarizing stimuli. Furthermore, given the lack of effect of TP-10 on SNr+ MSNs, we speculate that PDE10A inhibition may have a greater facilitatory effect on corticostriatal synaptic activity in striatopallidal MSNs. These data support further investigation of selective targeting of PDE signaling pathways in MSN subpopulations, as this may represent a promising novel approach for treating brain disorders involving dysfunctional glutamatergic and dopaminergic neurotransmission.

## Introduction

The basal ganglia form a circuit of subcortical nuclei involved in the implicit planning and execution of cognitive, motor, and emotional repertoires (Graybiel, 2000; Wilson, 2004). Dysfunctional neurotransmission in this circuit is implicated in the pathophysiology of many brain disorders, notably Parkinson's disease, Huntington's disease, Tourette syndrome, schizophrenia, and substance abuse (Kapur, 2004; Everitt and Robbins, 2005; DeLong and Wichmann, 2007). Thus, there is considerable interest in manipulating the basal ganglia circuit as a means towards novel therapies to treat these diseases. The focus of the present study is one promising target for such intervention, the cyclic nucleotide phosphodiesterase 10A (PDE10A), an enzyme highly enriched in the primary input neurons to the basal ganglia circuit, the striatal medium-sized spiny neurons (MSNs) (Menniti et al., 2007).

Striatal MSNs integrate information transmitted via cortical and thalamic glutamatergic afferents with input regarding salience from midbrain dopaminergic neurons (Surmeier et al., 2007). Striatal output is relayed by one of two pathways, the "direct" pathway involved in action selection and the "indirect" pathway involved in action suppression (Wilson, 2004; DeLong and Wichmann, 2007). MSNs of the direct pathway primarily express dopamine D1 receptors positively coupled to adenylyl cyclase and project directly to the basal ganglia output nuclei, the substantia nigra pars reticulata (SNr) and internal globus pallidus (GPi). MSNs of the indirect pathway primarily express dopamine D2 receptors negatively coupled to adenylyl cyclase and connect with the output nuclei by way of the external globus pallidus (GPe) and subthalamic nucleus.

The effects of dopamine D1 and D2 receptors on the activity of MSNs in both output pathways are mediated by both cAMP and cGMP (Greengard, 2001). Cyclic nucleotide

signaling also plays a key role in the regulation of synaptic plasticity at corticostriatal synapses (Calabresi et al., 2000) and in gene expression within MSNs (Berke et al., 1998). Although the role of cAMP in MSN function has received the most attention (Colwell and Levine, 1995; Greengard, 2001; Nishi et al., 2008), recent studies have shown that cGMP signaling increases the membrane excitability and responsiveness of MSNs to corticostriatal inputs (West and Grace, 2004).

Cyclic nucleotide phosphodiesterases (PDEs) regulate both spatial and temporal components of cAMP and cGMP signaling within distinct subcellular compartments (Lugnier, 2006; Menniti et al., 2006). The PDEs are organized into eleven families based on sequence homology, substrate specificity, and regulation (Bender and Beavo, 2006; Lugnier, 2006). Seven PDE families are present at moderate to high levels of expression in the striatum (Menniti et al., 2006). In this regard, PDE10A is unique in that this dual substrate enzyme (Fujishige et al., 1999; Loughney et al., 1999; Soderling et al., 1999) is expressed at high levels only in striatal MSNs (Seeger et al., 2003; Coskran et al., 2006; Xie et al., 2006; Sano et al., 2008). Within the striatum, PDE10A is compartmentalized proximal to the plasma membrane of postsynaptic sites within MSN dendritic spines (Kotera et al., 2004; Xie et al., 2006; Sano et al., 2008) and, thus, is positioned to regulate post-synaptic cyclic nucleotide signaling involved in the integration of glutamatergic and dopaminergic neurotransmission. High PDE10A expression is also found in MSN axons/terminals in the SNr and external globus pallidus (Seeger et al., 2003).

Pharmacological inhibition of PDE10A results in significant increases in cAMP and cGMP levels and leads to the phosphorylation of PKA substrates including cAMP-response element-binding protein (CREB), extracellular receptor kinase (ERK), dopamine- and cAMP-regulated phosphoprotein of M.W. 32 kDa (DARPP-32), and GluR1 in striatal neurons (Siuciak

et al., 2006b; Nishi et al., 2008). Given the key role of these signaling pathways in both dopaminergic and glutamatergic transmission, the ability of PDE10A inhibitors to modulate MSN activity may be of particular therapeutic relevance to numerous brain disorders associated with dysfunctional striatal output (Menniti et al., 2006; Siuciak et al., 2006a; Siuciak et al., 2006b; Menniti et al., 2007; Schmidt et al., 2008). However, a direct investigation of the effect of PDE10A inhibition on the activity of MSNs has not yet been reported. Therefore, the goal of the current study was to characterize the effect of PDE10A inhibition on corticostriatal signaling and the activity of electrophysiologically identified MSNs recorded in the intact rat.

## Methods

### *Drugs*

Urethane, papaverine hydrochloride, and Cremophor EL were purchased from Sigma Chemical (St. Louis, MO, USA). 2-{4-[Pyridin-4-yl-1-(2,2,2-trifluoroethyl)-1H-pyrazol-3-yl]-phoxymethyl}-quinoline succinic acid (TP-10; (Schmidt et al., 2008)) was synthesized at Pfizer Global Research and Development (Groton, CT). All other reagents were of the highest grade commercially available.

### *Subjects and surgery*

Electrophysiological recordings were made from 51 male Sprague-Dawley (Harlan, Indianapolis, IN) rats weighing 253-372 grams. Prior to use, animals were housed two- or three-per cage under conditions of constant temperature (21-23°C) and maintained on a 12:12 hour light/dark cycle with food and water available *ad libitum*. All animal protocols were approved by the Rosalind Franklin University of Medicine and Science Institutional Animal Care and Use Committee and adhere to the *Guide for the Care and Use of Laboratory Animals* published by the USPHS. Prior to surgery, animals were deeply anesthetized with urethane (1.5 g/kg, i.p.) and placed in a stereotaxic apparatus (Narishige International USA Inc., East Meadow, NY or David Kopf Instruments, Tujunga, CA). The level of anesthesia was periodically verified via the hind limb compression reflex and maintained using supplemental administration of anesthesia as previously described (Sammur et al., 2007; Ondracek et al., 2008). Temperature was monitored

using a rectal probe and maintained at 37°C using a heating pad (VI-20F, Fintronics Inc, Orange, CT). To minimize pain or discomfort, a solution of lidocaine HCl (2%) and epinephrine (1:100,000) (Henry Schein, Melville, NY) was injected into the scalp (s.c.) in a volume of ~0.3ml and allowed to diffuse for several minutes. An incision (~2-4 cm) was then made in the scalp and burr holes (~2-3 mm in diameter) were drilled in the skull overlying the right hemisphere of the frontal cortex (coordinates: 3.0-4.0 mm anterior from bregma, 1.5-2.2 mm lateral from the midline) and dorsal striatum (coordinates: -0.5-2.0 mm anterior from bregma, 2.0-3.5 mm lateral from the midline). In experiments involving antidromic stimulation of the substantia nigra pars reticulata (SNr), an additional burr hole was made overlying the right hemisphere of the SNr (coordinates: 5 mm posterior from bregma, 2.5 mm lateral from the midline). The dura mater was resected and the stimulating and recording electrodes were lowered into the brain using a Narishige or Kopf micromanipulator. All coordinates were determined using a rat brain stereotaxic atlas (Paxinos and Watson, 1986).

### ***Electrical stimulation and antidromic activation***

Concentric bipolar stimulating electrodes were implanted in the frontal cortex ipsilateral or contralateral to the recording electrode as indicated below. Previous studies have shown that MSNs receive synaptic inputs from bilateral intratelencephalic cortical neurons (IT) which project to both the ipsilateral and contralateral striatum, as well as from axon collaterals derived from ipsilateral corticospinal neurons which give rise to the pyramidal tract (PT)(Wilson, 2004). Other work suggests that striatonigral neurons preferentially receive innervation from IT-type cells, whereas striatopallidal neurons receive more robust input from PT-type cells (Lei et al., 2004). Given the above, it is possible that striatal PDE10A inhibition could have differential

effects on excitatory responses evoked by IT and PT inputs. Thus, the impact of striatal PDE10A inhibition on cortically-evoked activity was examined using both ipsilateral and contralateral cortical stimulation to allow for comparisons between effects involving both IT and PT inputs, or only IT inputs, respectively. All experiments using TP-10 utilized ipsilateral stimulation. All experiments using papaverine utilized contralateral cortical stimulation. In experiments involving antidromic stimulation, a concentric bipolar stimulating electrode was also implanted ipsilaterally in the SNr (coordinates were within the same range as indicated above). Electrical stimuli with durations of 500  $\mu$ s and intensities between 0.25-1.5 mA were generated using a stimulator and photoelectric constant current/stimulus isolation unit (S88 stimulator with PSIU6F stimulus isolation unit, Grass Instruments, Quincy, MA) and delivered in single low frequency pulses (0.5 Hz) for duration of 100 seconds as previously described (Ondracek et al., 2008).

Antidromic stimulation of the SNr was used to identify striatonigral projection neurons (SNr+ MSNs) in studies using single-unit extracellular recordings and systemic administration of TP-10. The following criteria were used to determine if spikes evoked by SNr stimulation were antidromic in nature: (1) constant latency of observed spike response, (2) all-or-none property of antidromic spikes as determined using sub- and supra-threshold stimulus intensities, and (3) collision of the antidromic spikes with orthodromic spikes generated in MSNs via low frequency stimulation of corticostriatal afferents (see above and Mallet et al., 2005). Collisions which could be observed consistently over 10 consecutive trials using supra-threshold stimulus intensities were considered positive. The current intensity (0.2 to 1.5 mA) used in collision tests for antidromic stimulation of the 49 striatonigral neurons studied herein was derived from ranges reported in previous studies (Tepper et al., 1995; Mallet et al., 2005; Ballion et al., 2008).

Striatal neurons were considered unresponsive to antidromic stimulation of the SNr if their spike responses evoked by SNr stimulation did not meet the above criteria or if they exhibited no spike response to SNr stimulation when tested utilizing a maximal current intensity (1.5 mA).

Unfortunately, striatopallidal neurons cannot be reliably identified with this technique since electrical stimulation of the GPe is likely to activate fibers of passage projecting from striatonigral MSNs (Wilson, 2004). To minimize issues associated with antidromic stimulation and the generation of back-propagating action potentials, we only tested neurons for antidromic responses (by stimulating the SNr) after all other measures (spontaneous activity, cortical stimulation, etc) had been performed. Moreover, because of the low frequency of the stimulation (0.5 Hz) used in the antidromic technique and the time period between recordings of different cells (typically  $\geq 15$  min), it is unlikely that this procedure produced persistent changes in excitability that could have impacted on subsequent recordings.

### ***Extracellular recordings and local drug administration using reverse microdialysis***

Concentric microdialysis probes having 4 mm of exposed membrane (225  $\mu$ m diameter) were implanted into the striatum and reverse microdialysis was performed concurrently with electrophysiological recordings as previously described (West and Grace, 2004). Briefly, extracellular recording microelectrodes were manufactured from 2.0 mm o.d. borosilicate glass capillary tubing (WPI, New York, NY) using a vertical micropipette puller (model PE-21, Narishige) and recordings of cortically-evoked activity were performed as previously described (Ondracek et al., 2008). A between-subjects approach was used throughout. Striatal MSNs were isolated during single-pulse cortical stimulation as described above. Recordings were initiated ~2-3 hours after probe implantation. TP-10 was solublized in 10% Cremophor EL/ 90% saline

(0.9%) solution (500 x stock solution, 1 mM) which was then diluted to a final concentration of 2  $\mu$ M using artificial cerebral spinal fluid (aCSF). In control experiments, aCSF contained the same concentration of Cremophor EL/saline solution as used above in studies with TP-10. Papaverine (500  $\mu$ M) was made up in aCSF immediately prior to use. Previous *in vitro* studies have shown that papaverine is a potent and relatively selective inhibitor of PDE10A with an  $IC_{50}$  value of 36 nM and a selectivity ratio of at least 9-1 over other PDE isoforms (Siuciak et al., 2006b). Moreover, the relatively novel compound TP-10 has been shown to exhibit superior potency (an  $IC_{50}$  value of 0.3 nM) and greatly improved selectivity of at least 2,500-fold over other PDE isoforms and CNS targets (Schmidt et al., 2008). To our knowledge, this is the first study to reverse dialyze these compounds into the striatum. Thus, presumed effective doses of papaverine and TP-10 were derived from information described in the above studies. The concentration of drug in the tissue immediately adjacent to the probe is estimated to be ~10% of the concentration in the perfusion fluid, and substantially less at the soma of the neuron being recorded. In some studies, MSNs were initially recorded in the presence of aCSF vehicle and then subsequent cells were recorded following a switch to either papaverine (500  $\mu$ M) or TP-10 (2  $\mu$ M). In other studies, MSNs were recorded in the presence of either aCSF vehicle or drug for the duration of the experiment. Given that the mean magnitude of drug-induced changes in spike activity did not differ significantly using these approaches (data not shown), data were pooled. In all studies, aCSF or drug was infused at least 20 min prior to recording striatal neuron activity. Given the complexity of performing recordings concurrently with microdialysis, antidromic stimulation was not attempted in this subset of studies.

### ***Extracellular recordings and systemic drug administration***

In single-unit recording studies involving systemic administration of drugs, vehicle (10% Cremophor EL in 0.9% saline) or TP-10 (0.32 or 3.2 mg/kg) was injected at least 10 minutes prior to the recording session. Effective doses of TP-10 were derived from previous studies which have shown that the maximal dose of TP-10 used in the current study (3.2 mg/kg, s.c.) increased tissue cGMP and cAMP levels approximately 2-4 fold and that peak increases occurred between 1 and 3 h post-injection (Schmidt et al., 2008). The low dose of TP-10 (0.32 mg/kg, s.c) was chosen because it was shown to have threshold effects on tissue levels of both cGMP and cAMP (Schmidt et al., 2008). After isolation of a cell, the effects of separate trials (50 pulses each) of single pulse cortical stimulation (0.4, 0.6, 0.8 and 1.0 mA stimulation intensities) were recorded. Spontaneous (non-evoked) firing activity (~2-5 min) of each isolated cell was then recorded. Lastly, stimulation of the SNr was performed to determine whether the recorded cell exhibited antidromic responses as described above. Striatal neurons exhibiting spike characteristics resembling cholinergic (tonic or regular firing at a rate of ~1-4 Hz) or fast-spiking interneurons (respond to low intensity cortical stimulation with a high-frequency train of short duration (<0.9 ms) action potentials) (Mallet et al., 2005) were not included in the current data set.

### ***Data Analysis and Statistics***

Firing rate histograms were constructed (1.0 ms bins of 2 min epochs) from spontaneous activity recorded from cells in a post-stimulation epoch following administration of either drug

(papaverine/TP-10) or vehicle (Ondracek et al., 2008). Neurons were considered “quiescent” if they failed to fire an action potential over a 2 min baseline recording period (Ondracek et al., 2008). All neurons (spontaneously active and quiescent) were included in analyses of cortically-evoked activity and peri-stimulus time histograms were constructed (1.0 ms bins) for each cortical stimulation trial. Furthermore, spike probabilities were calculated by dividing the number of evoked action potentials (either 0 or 1 per pulse) by the number of stimuli delivered (Ondracek et al., 2008). Single-unit and group data were also summarized using spike latency and S.D. latency plots as indicated. The statistical significance of drug-induced changes in spike activity was determined using either a paired t-test, Fisher exact test or one/two-way analysis of variance (ANOVA) as indicated (Sigma Stat, Jandel). Also, a Bonferroni post-hoc test was used as indicated to determine which group(s) contributed to overall differences seen with ANOVA.

### ***Histology***

After completion of each experiment, rats were deeply anesthetized and perfused transcardially with ice-cold saline followed by 10% formalin in buffered phosphate (PB) (EMS, Hatfield, PA). Brains were removed and postfixed in formalin/sucrose solution (30%) and stored at 4°C until saturated. Brains were then sectioned into 50 µm coronal slices, mounted, and stained with Neutral red/Cresyl Violet (10:1) solution to enable histological assessment of stimulating and recording electrodes (Sammut et al., 2007).

## Results

### *Stimulating electrode, microdialysis probe and recording electrode placements*

All identified stimulating electrode tips were confirmed to lie in the frontal cortex between 2.7 and 4.7 mm anterior to bregma, 1.0 and 2.5 mm lateral to the midline, and 2.0 and 4.0 mm ventral to the skull. In studies involving antidromic stimulation of the SNr, stimulating electrode tips were confirmed to lie between 4.5 and 5.8 mm posterior to bregma, 1.8 and 2.9 mm lateral to the midline, and 7.5 and 8.5 mm ventral to the dural surface (Paxinos and Watson, 1986) (Figure 1). Identified placements for recording electrodes implanted into the striatum were verified to lie between 0.5 and 1.7 mm anterior to bregma, 2.4 and 3.5 mm lateral to the midline, and 3.5 and 7.2 mm ventral to the dural surface (Paxinos and Watson, 1986) (Figure 1). In studies with microdialysis, coordinates could not be determined for individual recording electrodes and microdialysis probes due to combined tissue damage of both implants. However, in all cases microelectrode tracks were observed to penetrate the corpus callosum at a trajectory which was angled towards the microdialysis probe track in the dorsocentral striatum.

### *Intrastriatal infusion of PDE10A inhibitors*

When assessed qualitatively, intrastriatal infusion of both PDE10A inhibitors appeared to increase the rate of spontaneous spike activity. However, the majority of cells recorded proximal to the microdialysis probe in all groups were not spontaneously active (see below). Thus, with the low overall mean and small number of spontaneously active cells, as well as the relative variability in this measure, the statistical power associated with these outcomes may have been insufficient to test this effect. Nonetheless, group comparisons revealed that the mean firing rate

was not significantly affected by intrastriatal infusion of either papaverine (500  $\mu$ M) ( $p>0.05$ ; t-test; vehicle firing rate:  $0.03 \pm 0.02$  Hz; papaverine firing rate:  $0.2 \pm 0.16$  Hz) or TP-10 (2  $\mu$ M) ( $p>0.05$ ; t-test; vehicle firing rate:  $0.004 \pm 0.002$  Hz; TP-10 firing rate:  $0.112 \pm 0.08$  Hz). The proportion of spontaneously active cells in each group did not differ in papaverine ( $p>0.05$ ; Fisher exact test; vehicle: 2 spontaneously firing, 6 quiescent; papaverine: 1 cell spontaneously firing, 10 cells quiescent) or TP-10 treated groups ( $p>0.05$ ; Fisher exact test; vehicle: 3 cells spontaneously firing, 9 cells quiescent; TP-10: 5 cells spontaneously firing, 14 cells quiescent) as compared to vehicle controls.

To examine the effects of local PDE10A inhibition on spike activity evoked by electrical stimulation of frontal cortical afferents, individual stimulation trials consisting of 50 single pulses each (0.5 Hz, 500  $\mu$ s) were delivered to the frontal cortex using multiple current amplitudes (0.5, 0.75, 1.0 mA). The order of stimulation trials was counter-balanced for stimulus intensity across cells (i.e., the trial order consisted of 0.5, 0.75, 1.0 mA or 1.0, 0.75, 0.5 mA and was alternated for each cell). Short latency spike activity evoked during repeated single-pulse stimulation of both the contralateral (Figure 2A,B) and ipsilateral (Figure 3A,B) frontal cortex was dependent on the level of current intensity following local administration of vehicle and both PDE10A inhibitors (papaverine:  $p<0.001$ ;  $F(2,51)=17.694$ , TP-10:  $p<0.001$ ;  $F(2,87)=7.961$ ; Two-way ANOVA with Bonferroni post-hoc test). Intrastriatal infusion of papaverine induced a stimulation intensity-dependent increase in both mean  $\pm$  S.E.M. spike probability (Figure 2C;  $p<0.001$ ;  $F(1,51)=21.322$ ; Two-way ANOVA) and the number of spikes elicited per stimulation trial compared to vehicle controls (Figure 2C;  $p<0.001$ ;  $F(1,51)=24.537$ ; Two-way ANOVA). However, no significant differences in spike latency (Figure 2C;  $p>0.05$ ; two-way ANOVA) or S.D. of spike latency (data not shown) of cells were observed following

intraatrial infusion of papaverine as compared to vehicle controls. Intraatrial infusion of the more potent and selective PDE10A inhibitor TP-10 (Schmidt et al., 2008) induced a robust stimulation intensity-dependent increase in both mean  $\pm$  S.E.M. spike probability (Figure 3C;  $p < 0.001$ ;  $F(1,87) = 26.965$ ; Two-way ANOVA) and the number of spikes elicited per stimulation trial as compared to vehicle controls (Figure 3C;  $p < 0.001$ ;  $F(1,87) = 35.624$ ; Two-way ANOVA). In addition, intraatrial infusion of TP-10 significantly decreased the onset latency of cortically-evoked spikes in a stimulus intensity-dependent manner as compared to vehicle controls (Figure 3C;  $p < 0.005$ ;  $F(1,79) = 9.040$ ; Two-way ANOVA). No significant difference in the S.D. of spike latency (data not shown) was observed following intraatrial infusion of TP-10 as compared to vehicle controls, similar to outcomes with papaverine.

### ***Systemic PDE10A inhibitor administration***

As described above, the impact of PDE10A inhibition on cortically-evoked activity and spontaneous firing (recorded post-stimulation) was determined using a between-subjects design. In all cases recordings were performed  $\geq 10$  min after systemic administration (s.c.) of vehicle (10% Cremophor EL in 0.9% saline) or the selective PDE10A inhibitor TP-10 (0.32 or 3.2 mg/kg). No significant differences in the mean  $\pm$  S.E.M. time of recording (post-injection) existed between groups ( $p > 0.05$ ; unpaired t-test; vehicle:  $72 \pm 8$  min; TP-10:  $92 \pm 8$  min). Spontaneous spike activity (recorded post-stimulation) was not significantly altered following administration of either dose of TP-10 ( $p > 0.05$ ; One-way ANOVA; vehicle firing rate:  $0.009 \pm 0.003$  Hz; 0.32 mg/kg TP-10 firing rate:  $0.08 \pm 0.05$  Hz; 3.2 mg/kg TP-10 firing rate:  $0.03 \pm 0.01$  Hz) as compared to vehicle treated controls. The proportion of spontaneously active cells in each group did not differ across vehicle and TP-10 treated animals ( $p > 0.05$ ; Fisher exact test;

vehicle: 14 cells spontaneously firing, 38 cells quiescent; 0.32 mg/kg TP-10: 11 cells spontaneously firing, 33 cells quiescent; 3.2 mg/kg TP-10: 13 cells spontaneously firing, 39 cells quiescent).

Short latency spike activity evoked during repeated single-pulse stimulation of the ipsilateral frontal cortex was dependent on the level of current intensity following systemic administration of vehicle and both doses of TP-10 (Figure 4A-E;  $p < 0.001$ ;  $F(3,558) = 64.147$ ; Two-way ANOVA). A significant decrease in spike latency was also observed in all groups in response to increasing stimulation intensities (Figure 4A,B,D;  $p < 0.001$ ;  $F(3,468) = 12.768$ ; Two-way ANOVA). No significant changes in the S.D. of spike latency were observed with increasing stimulation intensities (Figure 4E;  $p > 0.05$ ; Two-way ANOVA). Systemic administration of both doses of TP-10 (3.2 and 0.32 mg/kg, s.c.) significantly increased the probability of observing cortically-evoked spike activity in a stimulation intensity-dependent manner as compared to vehicle treated controls (Figure 4A-C;  $p < 0.005$ ;  $F(2,558) = 11.909$ ; Two-way ANOVA). However, post-hoc comparisons of the effects of the low dose of TP-10 revealed a strong trend towards an increase in spike probability only at the 0.40 mA intensity, but this did not reach statistical significance ( $p = 0.078$ ). Furthermore, both doses of TP-10 significantly decreased the mean onset latency of cortically-evoked spikes in a stimulus intensity-dependent manner (Figure 4A,B,D;  $p < 0.001$ ;  $F(2,468) = 9.275$ ; Two-way ANOVA). The S.D. of spike latency was also decreased in a stimulus intensity-dependent manner following systemic administration of the higher (but not the lower) dose of TP-10 as compared to vehicle treated controls (Figure 4E;  $p < 0.001$ ;  $F(2,440) = 10.286$ ; Two-way ANOVA).

### ***PDE10A inhibition in MSN subpopulations***

The above data sets from vehicle and TP-10 (3.2 mg/kg, s.c.) treated animals were divided according to whether cells responded to antidromic activation of the SNr. Only recordings from animals in which the stimulating electrode placement could be confirmed to lie in the SNr were included in this study. Examples of antidromic responses elicited during SNr stimulation are shown in Figure 5A. Neurons that responded were designated SNr+ neurons and those that failed to respond to this stimulus were designated SNr- MSNs (Mallet et al., 2005; Ballion et al., 2008)(Figure 5A). Following TP-10 administration, identified SNr+ MSNs exhibited cortically-evoked spike activity which was indistinguishable from vehicle treated controls (Figure 5B;  $p>0.05$ ; Two-way ANOVA). However, a robust increase in spike probability was observed in SNr- MSNs following systemic administration of TP-10 (Figure 5B;  $p<0.001$ ;  $F(1,220)=31.413$ ; Two-way ANOVA) as compared to vehicle treated controls. Furthermore, a dose-dependent decrease in the onset latency of cortically-evoked spikes was observed following systemic administration of TP-10 in SNr- (Figure 5C;  $p<0.001$ ;  $F(1,186)=13.151$ ; Two-way ANOVA) but not SNr+ MSNs ( $p>0.05$ ; Two-way ANOVA) compared to vehicle treated controls. In addition, an overall group decrease in the S.D. of spike latency was observed in SNr- MSNs following systemically administered TP-10 (Figure 5D;  $p=0.009$ ;  $F(1,169)=6.995$ ; Two-way ANOVA) but not SNr+ MSNs ( $p>0.05$ ; Two-way ANOVA) compared to vehicle treated controls.

There was a significant increase in the incidence of antidromically activated (i.e., SNr+) MSNs following administration of TP-10 (Table 1;  $p=0.001$ ; Fisher Exact test). However, in contrast to SNr- MSNs, identified SNr+ MSNs from animals treated with TP-10 exhibited cortically-evoked spike activity that was indistinguishable from vehicle treated controls (Figure

5B;  $p>0.05$ ; two-way ANOVA). There was also no effect of TP-10 administration on evoked spike latency ( $p>0.05$ ; two-way ANOVA) or S.D. of spike latency in SNr+ MSNs. The average current intensity required to antidromically activate cells also did not differ across groups ( $p>0.05$ ; unpaired t-test; vehicle:  $0.71 \pm 0.17$  mA; 3.2 mg/kg TP-10:  $0.67 \pm 0.13$  mA). Thus, other than the increase in number detected, there was no apparent effect of PDE10A inhibition on other measures of evoked spike activity of SNr+ MSNs.

The increased incidence of antidromically activated (SNr+) cells observed following systemic TP-10 treatment indicated that the lack of effect of TP-10 on cortically-evoked activity in these cells (see Figure 5B, left) may have resulted from a sampling artifact induced by the antidromic stimulation procedure. Specifically, it is possible that with vehicle administration, the antidromic procedure preferentially samples from a population of the more excitable SNr+ MSNs. Following TP-10 administration, previously quiescent striatonigral neurons may become more excitable and more responsive to antidromic stimulation. If these previously quiescent neurons were less responsive to cortical stimulation than the more excitable population detected under control conditions, the inclusion of these MSNs in the SNr+ data set following TP-10 treatment could decrease overall measures of spike probability within the SNr+ MSNs in the TP-10 group, thus masking potential excitatory effects of drug. Indeed, in vehicle treated animals there was a small increase in the spike probability in the antidromically activated (SNr+) MSNs compared to those that were not antidromically activated; however, this failed to reach statistical significance ( $p=0.09$ ; Two-way ANOVA). To examine this possibility further, we compared the spike probability distributions of neurons that were antidromically activated (SNr+ MSNs) with those that were not activated (SNr- MSNs) from animals treated with vehicle or TP-10 (Figure 6). The apparent lack of an increase in the relative percentage of SNr+ MSNs exhibiting lower

spike probabilities following TP-10 administration (Figure 6, left) indicates that the antidromic activation procedure did not induce a sampling artifact. Additionally, comparisons of cortically-evoked activity in vehicle treated animals from the SNr+ and SNr- MSN groups do not show significant differences in spike probability distribution across vehicle groups. However, the percentage of SNr- MSNs exhibiting high spike probabilities (0.9-1.0) during cortical stimulation was substantially increased in TP-10 treated animals as compared to vehicle controls (Figure 6, right).

## Discussion

PDE10A is highly expressed in striatal MSNs, regulating both cGMP and cAMP signaling (Menniti et al., 2007). The results of the present study indicate that pharmacological inhibition of PDE10A increases the responsiveness of MSNs to excitatory corticostriatal input. Increases in cortically-evoked activity were consistently observed in studies using two relatively selective PDE10A inhibitors delivered either via intrastriatal infusion or systemic administration. In a subset of studies we were able to categorize striatal neurons as either striatonigral (SNr+ MSNs) or unidentified (SNr- MSNs) using antidromic activation techniques. Our findings suggest that PDE10A inhibition has a greater facilitatory effect on cortically-evoked activity in the SNr- MSN group which is likely to be composed primarily of striatopallidal cells.

### *PDE10A inhibition increases excitability of MSNs in response to corticostriatal input*

Previous studies have shown that drugs that augment cAMP or cGMP levels in MSNs increase measures of corticostriatal transmission (Colwell and Levine, 1995; West and Grace, 2004). Results from biochemical studies suggest that PDE10A inhibition may enhance striatal MSN activity in a similar manner (Nishi et al., 2008). This hypothesis was examined directly in the current study by measuring the effects of PDE10A inhibition on MSN single-unit activity following cortical stimulation in anesthetized rats (Ondracek et al., 2008). Intrastriatal infusion of the PDE10A inhibitors papaverine (500  $\mu$ M) or TP-10 (2  $\mu$ M) during cortical stimulation increased MSN spike probability and total number of spikes per stimulation. Infusion of TP-10, but not papaverine, also decreased the onset latency of cortically-evoked spikes. Systemic administration of TP-10 had essentially identical effects. Both a low (0.32 mg/kg) and high (3.2 mg/kg) subcutaneous dose of TP-10 decreased the onset latency of cortically-evoked spikes. The

higher dose of TP-10 also increased the probability of evoking spike activity across multiple stimulation intensities. Interestingly, a decrease in the variance of the onset latency of evoked spikes was observed following systemic administration of the high dose of TP-10, suggesting PDE10A inhibition temporally constrains cortically-evoked activity. Taken together, these results indicate that under physiological conditions, PDE10A activity may act to filter asynchronous or weak cortical input so that only strongly coherent corticostriatal transmission is communicated by MSN spike activity to postsynaptic targets in the globus pallidus and SNr.

With the exception of effects on spike latency, intrastriatal infusion of papaverine and TP-10 had qualitatively similar effects on spike responses evoked by ipsilateral and contralateral stimulation of the frontal cortex. Differences in spike probability and onset latency were apparent between the control groups in these studies, however, this is likely due to the differences in anatomical and physiological properties of intratelencephalic (IT) and pyramidal tract (PT) cortical projections (Wilson, 2004). However, it is currently unclear whether the more robust effect of TP-10 on spike latency resulted from differential drug effects on responsiveness to IT and PT inputs or differences in the potency of PDE10A inhibition produced by TP-10 and papaverine (see above). Future studies will be needed to address this issue. In any event, striatal PDE10A inhibition is likely to augment the responsiveness of striatal MSNs to both IT and PT type corticostriatal inputs.

PDE10A is selectively expressed in striatopallidal and striatonigral MSNs but is not found in striatal interneurons (Xie et al., 2006; Sano et al., 2008). Furthermore, results from immuno-electron microscopy studies indicate the enzyme is localized to dendrites and spines of MSNs but not to elements pre-synaptic to these structures. Thus, it is highly likely that the facilitatory effects of PDE10A inhibition on corticostriatal transmission occur at the level of the

MSN. In this context, it is interesting that the concentration response relationship for affecting the onset latency of cortically evoked spikes appears to differ after striatal and systemic exposure to PDE10A inhibitors. TP-10 is a highly potent and selective PDE10A inhibitor. The 3.2 mg/kg dose used in the present study induces near maximal increase in striatal cGMP and cAMP concentrations at free exposures consistent with high selectivity for PDE10A inhibition, whereas the low dose (0.32 mg/kg) is at the threshold for induction of such biochemical effects (Schmidt et al., 2008). The fact that the low TP-10 dose elicited only a decrease in spike onset latency suggests that this parameter is the most sensitive to PDE10A inhibition. Interestingly, TP-10, but not papaverine, decreased onset latency after intrastriatal infusion. The exact concentrations of drug exposure of the recorded neurons cannot be determined after reverse dialysis. Nonetheless, an explanation for the difference is that TP-10 infusion at 2  $\mu$ M results in a greater level of PDE10A inhibition than that produced by papaverine at 500  $\mu$ M. This interpretation is consistent with the ~200-fold higher potency of TP-10 for PDE10A inhibition. Thus, paradoxically, spike latency is the least sensitive to PDE10A inhibition following direct striatal infusion of the inhibitors. This paradox may be an intimation of effects of PDE10A inhibition that are 'second order' to effects on individual MSNs. Striatal infusion impacts only a small fraction of MSNs and this fraction is unlikely to affect the basal ganglia circuit sufficiently to directly feedback on the recorded neurons. In contrast, PDE10A inhibition after systemic administration reflects direct effects of the inhibitor on the recorded neuron coupled with circuit level effects summing over all the MSNs. We speculate that these latter circuit level effects may increase the sensitivity of spike latency to PDE10A inhibition after systemic administration.

### ***Differential effects of PDE10A inhibition on MSN subpopulations***

An interesting finding in the present study is a differential sensitivity of striatal projection neurons to PDE10A inhibition. Thus, the effects of TP-10 administration on cortically-evoked activity described above occurred only in neurons categorized as SNr- MSNs. Because the success rate of the antidromic procedure increased to approximately 50% in the presence of TP-10, it can be assumed that the SNr- MSN group was composed almost entirely of striatopallidal neurons under these conditions (i.e., each projection pathway makes up approximately 50% of striatal output cells, see Bolam et al., 2000, for review). This interpretation is strongly supported by recent studies by Snyder and colleagues showing that papaverine increases DARPP-32 phosphorylation much more robustly in identified striatopallidal as compared to striatonigral MSNs (Nishi et al., 2008).

There is no evidence for differential expression of PDE10A mRNA or protein in striatopallidal or striatonigral MSNs (Seeger et al., 2003; Coskran et al., 2006; Xie et al., 2006; Sano et al., 2008). Thus, a more likely explanation for the preferential effect of PDE10A inhibition on striatopallidal cells derives from the inherent neuroanatomical and electrophysiological differences between striatopallidal and striatonigral MSNs. D2-expressing striatopallidal MSNs receive more robust cortical innervation (Lei et al., 2004) and exhibit larger and more frequent responses to excitatory synaptic inputs than D1-expressing striatonigral MSNs (Kreitzer and Malenka, 2007; Cepeda et al., 2008). Furthermore, striatopallidal cells appear to be more responsive to depolarizing current injections than D1-expressing MSNs (Kreitzer and Malenka, 2007; Cepeda et al., 2008), a property that has recently been attributed to their significantly smaller dendritic tree (Gertler et al., 2008). Given this, it is not unexpected that

blockade of cyclic nucleotide breakdown following PDE10A inhibition would have a larger impact on cortically-evoked activity in striatopallidal versus striatonigral MSNs.

While speculative, the present results also suggest that PDE10A inhibition may increase the axonal/terminal excitability of MSNs. Systemic administration of TP-10 increased the number of antidromically activated (SNr+) MSNs. A parsimonious explanation for this observation is an increase in axonal excitability, since there was no significant effect of TP-10 on responsiveness to cortical stimulation in this SNr+ MSN population. Additional studies will be needed to directly test this hypothesis as we did not perform current amplitude/antidromic response curves in the current study. However, PDE10A is transported to MSN axons and terminals and the terminal concentration of the protein appears to be at least as high as in striatum, based on Western blot analysis (Seeger et al., 2003). Thus, these findings further support the hypothesis that PDE10A inhibition increases striatal output, in this case potentially via the direct facilitation of axonal excitability.

### ***Implications for the treatment of neuropsychiatric disorders***

Abnormal striatal output resulting from dysfunctional striatopallidal transmission is thought to contribute significantly to the pathophysiology of schizophrenia, Parkinson's disease, Huntington's disease and Tourette syndrome (Winterer and Weinberger, 2004; Groenewegen et al, 2003; DeLong and Wichmann, 2007). Thus, the ability of PDE10A inhibitors to enhance striatopallidal MSN activation may be of particular therapeutic relevance to some of these diseases (Menniti et al 2007; Menniti et al 2006; Schmidt et al 2008; Siuciak et al 2006a; Siuciak et al 2006b). PDE10A inhibition is associated with a number of behavioral effects in rodents including reduced conditioned-avoidance responding and hyperactivity induced by the

psychostimulants phencyclidine and amphetamine (Schmidt et al 2008; Siuciak et al 2006a). The data presented herein may reveal a physiological basis for these behavioral effects of PDE10A inhibitors, specifically, increased responsiveness of striatopallidal MSNs to cortical input. Indeed, the behavioral profile of PDE10A inhibitors in these assays strongly resembles that of dopamine D2 receptor antagonists (Schmidt et al 2008), which act to disinhibit the D2-expressing striatopallidal MSNs (see Surmeier et al., 2007, for review). Nonetheless, PDE10A inhibitors also differ significantly from D2 receptor antagonists in other preclinical behavioral models such as the induction of catalepsy and prepulse inhibition of startle (Schmidt et al 2008). These differences may reflect the fact that PDE10A also regulates the activity of striatonigral pathway neurons, as revealed in the current study using antidromic activation techniques as an apparent increase in axonal excitability of SNr+ neurons. Thus, it will be of considerable interest to continue to compare the physiological effects of PDE10A inhibitors with D2 receptor antagonists in preparation for interpreting the behavioral and therapeutic profile of PDE10A inhibitors in patients with schizophrenia and other neuropsychiatric disorders. Finally, given that PDE10A is capable of hydrolyzing both cAMP and cGMP, future studies will be needed to elucidate the individual roles that cAMP and cGMP play in the facilitation of corticostriatal-striatopallidal throughput observed following striatal PDE10A inhibition.

## Acknowledgments

The authors thank Drs. Marjorie A. Ariano and Robin Kleiman for helpful discussions during the design of these experiments.

## References

- Ballion B, Mallet N, Bezard E, Lanciego JL and Gonon F (2008) Intratelencephalic corticostriatal neurons equally excite striatonigral and striatopallidal neurons and their discharge activity is selectively reduced in experimental parkinsonism. *Eur J Neurosci* **27**:2313-2321.
- Bender AT and Beavo JA (2006) Cyclic nucleotide phosphodiesterases: molecular regulation to clinical use. *Pharmacol Rev* **58**:488-520.
- Berke JD, Paletzki RF, Aronson GJ, Hyman SE and Gerfen CR (1998) A complex program of striatal gene expression induced by dopaminergic stimulation. *J Neurosci* **18**:5301-5310.
- Bolam JP, Hanley JJ, Booth PA and Bevan MD (2000) Synaptic organisation of the basal ganglia. *J Anat* **196** ( Pt 4):527-542.
- Calabresi P, Gubellini P, Centonze D, Picconi B, Bernardi G, Chergui K, Svenningsson P, Fienberg AA and Greengard P (2000) Dopamine and cAMP-regulated phosphoprotein 32 kDa controls both striatal long-term depression and long-term potentiation, opposing forms of synaptic plasticity. *J Neurosci* **20**:8443-8451.
- Cepeda C, Andre VM, Yamazaki I, Wu N, Kleiman-Weiner M and Levine MS (2008) Differential electrophysiological properties of dopamine D1 and D2 receptor-containing striatal medium-sized spiny neurons. *Eur J Neurosci* **27**:671-682.
- Colwell CS and Levine MS (1995) Excitatory synaptic transmission in neostriatal neurons: Regulation by cyclic AMP-dependent mechanisms. *J Neurosci* **15**:1704-1713.
- Coskran TM, Morton D, Menniti FS, Adamowicz WO, Kleiman RJ, Ryan AM, Strick CA, Schmidt CJ and Stephenson DT (2006) Immunohistochemical localization of

- phosphodiesterase 10A in multiple mammalian species. *J Histochem Cytochem* **54**:1205-1213.
- DeLong M and Wichmann T (2007) Circuits and circuit disorders of the basal ganglia. *Arch Neurol* **64**:20-24.
- Everitt BJ and Robbins TW (2005) Neural systems of reinforcement for drug addiction: from actions to habits to compulsion, *Nat Neurosci* **8**: 1481-1489.
- Fujishige K, Kotera J and Omori K (1999) Striatum- and testis-specific phosphodiesterase PDE10A isolation and characterization of a rat PDE10A. *Eur J Biochem* **266**:1118-1127.
- Gertler TS, Chan CS, and Surmeier DJ (2008) Dichotomous anatomical properties of adult striatal medium spiny neurons. *J Neurosci* **28**:10814-10824.
- Graybiel AM (2000) The basal ganglia. *Curr Biol* **10**:R509-511.
- Greengard P (2001) The neurobiology of slow synaptic transmission. *Science* **294**:1024-1030.
- Groenewegen HJ, van den Heuvel OA, Cath DC, Voorn P and Veltman DJ (2003) Does an imbalance between the dorsal and ventral striatopallidal systems play a role in Tourette's syndrome? A neuronal circuit approach. *Brain Dev* **25**:S3-S14.
- Kapur S (2004) How antipsychotics become anti-'psychotic'-from dopamine to salience to psychosis. *Trends Neurosci* **25**:402-406.
- Kotera J, Sasaki T, Kobayashi T, Fujishige K, Yamashita Y and Omori K (2004) Subcellular localization of cyclic nucleotide phosphodiesterase type 10A variants, and alteration of the localization by cAMP-dependent protein kinase-dependent phosphorylation. *J Biol Chem* **279**:4366-4375.
- Kreitzer AC and Malenka RC (2007) Endocannabinoid-mediated rescue of striatal LTD and motor deficits in Parkinson's disease models. *Nature* **445**:643-647.

- Lei W, Jiao Y, Del Mar N and Reiner A (2004) Evidence for differential cortical input to direct pathway versus indirect pathway striatal projection neurons in rats. *J Neurosci* **24**:8289-8299.
- Loughney K, Snyder PB, Uher L, Rosman GJ, Ferguson K and Florio VA (1999) Isolation and characterization of PDE10A, a novel human 3', 5'-cyclic nucleotide phosphodiesterase. *Gene* **234**:109-117.
- Lugnier C (2006) Cyclic nucleotide phosphodiesterase (PDE) superfamily: a new target for the development of specific therapeutic agents. *Pharmacol Ther* **109**:366-398.
- Mallet N, Le Moine C, Charpier S and Gonon F (2005) Feedforward inhibition of projection neurons by fast-spiking GABA interneurons in the rat striatum in vivo. *J Neurosci* **25**:3857-3869.
- Menniti FS, Chappie TA, Humphrey JM and Schmidt CJ (2007) Phosphodiesterase 10A inhibitors: a novel approach to the treatment of the symptoms of schizophrenia. *Curr Opin Investig Drugs* **8**:54-59.
- Menniti FS, Faraci WS and Schmidt CJ (2006) Phosphodiesterases in the CNS: targets for drug development. *Nat Rev Drug Discov* **5**:660-670.
- Nishi A, Kuroiwa M, Miller DB, O'Callaghan JP, Bateup HS, Shuto T, Sotogaku N, Fukuda T, Heintz N, Greengard P and Snyder GL (2008) Distinct roles of PDE4 and PDE10A in the regulation of cAMP/PKA signaling in the striatum. *J Neurosci* **28**:10460-10471.
- Ondracek JM, Dec A, Hoque KE, Lim SA, Rasouli G, Indorkar RP, Linardakis J, Klika B, Mukherji SJ, Burnazi M, Threlfell S, Sammut S and West AR (2008) Feed-forward excitation of striatal neuron activity by frontal cortical activation of nitric oxide signaling in vivo. *Eur J Neurosci* **27**:1739-1754

- Paxinos G and Watson C (1986) The rat brain in stereotaxic coordinates. *Academic Press, New York*.
- Sammut S, Park DJ and West AR (2007) Frontal cortical afferents facilitate striatal nitric oxide transmission in vivo via a NMDA receptor and neuronal NOS-dependent mechanism. *J Neurochem* **103**:1145-1156.
- Sano H, Nagai Y, Miyakawa T, Shigemoto R and Yokoi M (2008) Increased social interaction in mice deficient of the striatal medium spiny neuron-specific phosphodiesterase 10A2. *J Neurochem*.
- Schmidt CJ, Chapin DS, Cianfrogna J, Corman ML, Hajos M, Harms JF, Hoffman WE, Lebel LA, McCarthy SA, Nelson FR, Proulx-Lafrance C, Majchrzak MJ, Ramirez AD, Schmidt K, Seymour PA, Siuciak JA, Tingley Iii FD, Williams RD, Verhoest PR and Menniti FS (2008) Preclinical characterization of selective PDE10A inhibitors: A new therapeutic approach to the treatment of schizophrenia. *J Pharmacol Exp Ther*.
- Seeger TF, Bartlett B, Coskran TM, Culp JS, James LC, Krull DL, Lanfear J, Ryan AM, Schmidt CJ, Strick CA, Varghese AH, Williams RD, Wylie PG and Menniti FS (2003) Immunohistochemical localization of PDE10A in the rat brain. *Brain Res* **985**:113-126.
- Siuciak JA, Chapin DS, Harms JF, Lebel LA, McCarthy SA, Chambers L, Shrikhande A, Wong S, Menniti FS and Schmidt CJ (2006a) Inhibition of the striatum-enriched phosphodiesterase PDE10A: a novel approach to the treatment of psychosis. *Neuropharmacology* **51**:386-396.
- Siuciak JA, McCarthy SA, Chapin DS, Fujiwara RA, James LC, Williams RD, Stock JL, McNeish JD, Strick CA, Menniti FS and Schmidt CJ (2006b) Genetic deletion of the

striatum-enriched phosphodiesterase PDE10A: evidence for altered striatal function.

*Neuropharmacology* **51**:374-385.

Soderling SH, Bayuga SJ, and Beavo JA (1999) Isolation and characterization of a dual-substrate phosphodiesterase gene family: PDE10A. *Proc Natl Acad Sci U S A* **96**:7071-7076.

Surmeier DJ, Ding J, Day M, Wang Z, Shen W (2007) D1 and D2 dopamine-receptor modulation of striatal glutamatergic signaling in striatal medium spiny neurons. *Trends Neurosci* **30**:228-35.

Tepper JM, Martin LP and Anderson DR (1995) GABA<sub>A</sub> receptor-mediated inhibition of rat substantia nigra dopaminergic neurons by pars reticulata projection neurons. *J Neurosci* **15**:3092-3103.

West AR and Grace AA (2004) The nitric oxide-guanylyl cyclase signaling pathway modulates membrane activity States and electrophysiological properties of striatal medium spiny neurons recorded in vivo. *J Neurosci* **24**:1924-1935.

Wilson CJ (2004) *Basal Ganglia*. Oxford University Press, Oxford.

Winterer G and Weinberger DR (2004) Genes, dopamine and cortical signal-to-noise ratio in schizophrenia. *Trends Neurosci* **27**:683-690.

Xie Z, Adamowicz WO, Eldred WD, Jakowski AB, Kleiman RJ, Morton DG, Stephenson DT, Strick CA, Williams RD and Menniti FS (2006) Cellular and subcellular localization of PDE10A, a striatum-enriched phosphodiesterase. *Neuroscience* **139**:597-607.

## Footnotes:

a) This work was supported by the Chicago Medical School, the National Alliance for Research on Schizophrenia and Depression, Pfizer Incorporated, and by a United States Public Health Service Grant [NS 047452].

b) Send reprint requests to: Dr. Anthony R. West, Dept. of Neuroscience, Rosalind Franklin University of Medicine and Science, Department of Neuroscience, 3333 Green Bay Road, North Chicago, IL 60064, USA. [Anthony.west@rosalindfranklin.edu](mailto:Anthony.west@rosalindfranklin.edu)

c) <sup>1</sup> Dept. of Neuroscience, Rosalind Franklin University of Medicine and Science, 3333 Green Bay Road, North Chicago, IL, 60064, USA

<sup>2</sup> Pfizer Global Research and Development, Eastern Point Road, Groton, CT, 06340, USA

## Legends for figures

**Figure 1. Position of implants in the frontal cortex, dorsal striatum and SNr.** **A)** Stimulating electrodes were implanted into the frontal cortex (see Materials and Methods). **B)** Electrophysiological recording electrodes were implanted into the dorsocentral striatum. **C)** In studies involving antidromic stimulation of the SNr, stimulating electrodes were implanted into the SNr. The large unfilled arrows ( $\Rightarrow$ ) indicate the termination sites of implants in the frontal cortex, dorsal striatum and SNr. Abbreviations: aC, anterior commissure; aON, anterior olfactory nucleus; FCx, frontal cortex; CPu, caudate putamen; CC, corpus callosum; HC, hippocampus; IV, lateral ventricle; SNr, substantia nigra pars reticulata; SNc, substantia nigra pars compacta; d, dorsal; m, medial

**Figure 2. Intrastriatal infusion of the PDE10A inhibitor papaverine increases the responsiveness of striatal neurons to electrical stimulation of the contralateral frontal cortex.** **A) Top:** Representative traces of cortically-evoked spike activity of a single-unit recorded following intrastriatal vehicle infusion. **Bottom:** Corresponding peri-stimulus time interval histogram showing the response of the same striatal neuron to cortex stimulation delivered over 50 stimulation trials. **B) Top:** Representative traces of cortically-evoked spike activity of a single-unit recorded following local papaverine (500  $\mu$ M) infusion. **Bottom:** Corresponding peri-stimulus time interval histogram showing the response of the same striatal neuron to cortex stimulation delivered over 50 stimulation trials. For both A) and B), ten superimposed traces of cortically-evoked spike responses from a single striatal neuron are shown for trials delivered at the 1.0 mA stimulus intensity. Arrow indicates the location of the stimulus artifact. **C) Top:** Cortical stimulation induced a stimulus intensity-dependent increase in spike

probability during both aCSF and papaverine infusion ( $p < 0.001$ ; two-way ANOVA,  $n = 8-11$  cells;  $N = 7-8$  rats). However, papaverine (500  $\mu\text{M}$ ) infusion significantly increased the mean  $\pm$  S.E.M. probability of eliciting spike activity during cortical stimulation as compared to cells recorded during aCSF infusion ( $p < 0.001$ ; two-way ANOVA with Bonferroni t-test;  $**p < 0.01$  for trials using 0.5 and 0.75 mA stimulus intensities;  $n = 8-11$  cells;  $N = 7-8$  rats). *Middle:* Papaverine infusion significantly increased the mean  $\pm$  S.E.M. number of spikes evoked per trial (50 stimulus pulses) as compared to cells recorded during aCSF infusion ( $p < 0.001$ ; two-way ANOVA with Bonferroni t-test;  $**p < 0.01$  for trials using 0.5 and 0.75 mA stimulus intensities;  $*p < 0.05$  for trials using 1.0 mA stimulus intensities;  $n = 8-11$  cells;  $N = 7-8$  rats). *Bottom:* Papaverine infusion did not affect the mean  $\pm$  S.E.M. onset latency of spike responses evoked during single pulse electrical stimulation of the frontal cortex as compared to cells recorded during aCSF infusion ( $p > 0.05$ ; two-way ANOVA).

**Figure 3. Intrastriatal infusion of the PDE10A inhibitor TP-10 increases the responsiveness of striatal neurons to electrical stimulation of the ipsilateral frontal cortex.**

**A) Top:** Representative traces of cortically-evoked spike activity of a single-unit recorded following intrastriatal vehicle infusion. *Bottom:* Corresponding peri-stimulus time interval histogram showing the response of the same striatal neuron to cortex stimulation delivered over 50 stimulation trials. **B) Top:** Representative traces of cortically-evoked spike activity of a single-unit recorded following local TP-10 (2  $\mu\text{M}$ ) infusion. *Bottom:* Corresponding peri-stimulus time interval histogram showing the response of the same striatal neuron to cortex stimulation delivered over 50 stimulation trials. For both A) and B), ten superimposed traces of cortically-evoked spike responses from a single striatal neuron are shown for trials delivered at

the 1.0 mA stimulus intensity. Arrow indicates the location of the stimulus artifact. **C) Top:** TP-10 (2  $\mu$ M) infusion significantly increased the mean  $\pm$  S.E.M. probability of eliciting spike activity during cortical stimulation as compared to cells recorded during aCSF infusion ( $p<0.001$ ; two-way ANOVA with Bonferroni t-test;  $*p<0.05$  for trials using 0.5 mA stimulus intensities;  $**p<0.01$  for trials using 0.75 and 1.0 mA stimulus intensities;  $n=12-19$  cells,  $N=6-8$  rats). **Middle:** TP-10 infusion significantly increased the mean  $\pm$  S.E.M. number of spikes evoked per trial (50 stimulus pulses) of cortical stimulation as compared to cells recorded during aCSF infusion ( $p<0.001$ ; two-way ANOVA with Bonferroni t-test;  $*p<0.05$  for trials using 0.5 mA stimulus intensities;  $**p<0.01$  for trials using 0.75 mA stimulus intensities;  $***p<0.001$  for trials using 1.0 mA stimulus intensities;  $n=12-19$  cells,  $N=6-8$  rats). **Bottom:** TP-10 infusion significantly increased the mean  $\pm$  S.E.M. onset latency of spike responses evoked during single pulse electrical stimulation of the frontal cortex as compared to cells recorded during aCSF infusion ( $p<0.001$ ; two-way ANOVA with Bonferroni t-test;  $*p<0.05$  for trials using 0.75 and 1.0 mA stimulus intensities;  $n=6-19$  cells,  $N=6-8$  rats).

**Figure 4. Systemic TP-10 administration increases the responsiveness of striatal neurons to electrical stimulation of the ipsilateral frontal cortex.** **A)** Representative traces of cortically-evoked spike activity of a single-unit recorded following systemic vehicle administration. *Inset:* Corresponding peri-stimulus time interval histogram showing the response of the same striatal neuron to cortex stimulation delivered over 50 stimulation trials. **B)** Representative traces of cortically-evoked spike activity of a single-unit recorded following systemic TP-10 (3.2 mg/kg, s.c.) administration. *Inset:* Corresponding peri-stimulus time interval histogram showing the response of the same striatal neuron to cortex stimulation delivered over 50 stimulation trials.

For both A) and B), ten superimposed traces of cortically-evoked spike responses from a single striatal neuron are shown for trials delivered at the 1.0 mA stimulus intensity. Arrow indicates the location of the stimulus artifact. **C)** A current intensity-dependent increase in the probability of evoking short latency spike activity during cortical stimulation was observed following TP-10 administration as compared to vehicle treated controls ( $p < 0.001$ ; Two-way ANOVA with Bonferroni t-test,  $*p < 0.05$  for trials using 0.4, 0.8 and 1.0 mA stimulus intensities and 3.2 mg/kg TP-10). **D)** TP-10 administration significantly decreased the mean onset latency of cortically-evoked spikes in a stimulus intensity-dependent manner compared to vehicle treated controls ( $p < 0.001$ ; two-way ANOVA with Bonferroni t-test;  $^{\#}p < 0.05$  for trials using 0.4 mA stimulus intensities and 0.32 mg/kg TP-10;  $*p < 0.05$  for trials using 0.8 and 1.0 mA stimulus intensities and 3.2 mg/kg TP-10). **E)** TP-10 administration significantly decreased mean S.D. of spike latency compared to vehicle ( $p < 0.001$ ; two-way ANOVA with Bonferroni t-test;  $*p < 0.05$  for the trial using the 0.8 mA stimulus intensity and 3.2 mg/kg TP-10). Data are derived from  $n = 41-52$  cells per group;  $N = 8-10$  rats per group.

**Figure 5. Effect of systemic TP-10 administration on cortically-evoked activity of identified striatonigral (SNr+) MSNs.** **A)** Representative recordings (10 overlaid traces) of orthodromic responses evoked via cortical stimulation (1), followed by constant latency responses to SNr stimulation (2). The collision test (3) is used to identify a striatonigral (SNr+ MSN) by antidromic activation. The SNr stimulation was delivered either 40 ms (no collision) or 15 ms (collision) after the delivery of the stimulus pulse to the frontal cortex (Mallet et al., 2005). Notice the antidromic spikes evoked by SNr stimulation exhibited fixed onset latencies, whereas the onset latency of cortically-evoked orthodromic spikes was relatively variable. **B) Left:** The

mean  $\pm$  S.E.M. spike probability observed in SNr+ MSNs was not changed following TP-10 administration as compared to vehicle controls ( $p>0.05$ ; two-way ANOVA). *Right:* A significant increase in the mean  $\pm$  S.E.M. spike probability was observed across all stimulus intensities in SNr- MSNs following TP-10 administration as compared to vehicle controls ( $p<0.001$ ; two-way ANOVA with Bonferroni t-test;  $*p<0.05$  for trials using 0.4 mA stimulus intensities;  $**p<0.01$  for trials using 0.6-1.0 mA stimulus intensities). **C) Left:** The mean  $\pm$  S.E.M. onset latency of cortically-evoked spikes observed in SNr+ MSNs was not changed following TP-10 administration as compared to vehicle controls ( $p>0.05$ ; two-way ANOVA). *Right:* A significant stimulus intensity-dependent decrease in the mean  $\pm$  S.E.M. onset latency of cortically-evoked spikes was observed in SNr- MSNs following TP-10 administration as compared to vehicle controls ( $p<0.001$ ; two-way ANOVA with Bonferroni t-test;  $*p<0.05$  for trials using 0.4, 0.8 and 1.0 mA stimulus intensities). **D) Left:** TP-10 administration did not affect the S.D. of onset latency of cortically-evoked spikes in SNr+ MSNs as compared to vehicle controls ( $p>0.05$ ; two-way ANOVA). *Right:* An overall significant decrease in the S.D. of onset latency of cortically-evoked spikes was observed in SNr- MSNs following TP-10 administration as compared to vehicle controls ( $p=0.009$ ; two-way ANOVA with Bonferroni t-test;  $p>0.05$  for trials using 0.4-1.0 mA stimulus intensities). Data are derived from  $n=15-37$  cells per group;  $N=7-9$  rats per group.

**Figure 6. Effect of TP-10 administration on the mean spike probability distribution of SNr+ and SNr- MSNs recorded during stimulation of the frontal cortex.** The average spike probability of SNr+ (left) and SNr- (right) MSNs in vehicle and TP-10 treated groups was determined across individual trials of cortical stimulation (**A-D**) performed using different

intensities of electrical stimulation (0.4-1.0 mA). The percentage of cells averaging a given spike probability in response to 50 stimulus pulses/trial was calculated and plotted across individual bins (increments of 0.1). Note that the rightward shift in the spike probability distribution in response to increased intensities of electrical stimulation is similar across vehicle and TP-10 treated SNr+ MSNs, whereas this shift occurs at lower current amplitudes and is more prominent across stimulation trials in TP-10 treated SNr- MSNs.

**Table 1. Effects of TP-10 on the relative proportion of striatal neurons exhibiting antidromic spikes in response to SNr stimulation**

	SNr+	SNr-
Vehicle	9	37
3.2 mg/kg TP-10	25 *	22

There was a significant increase in the number of SNr+ cells recorded following TP-10 administration compared to vehicle administration ( $p=0.001$ ; Fisher exact test).

Figure 1.

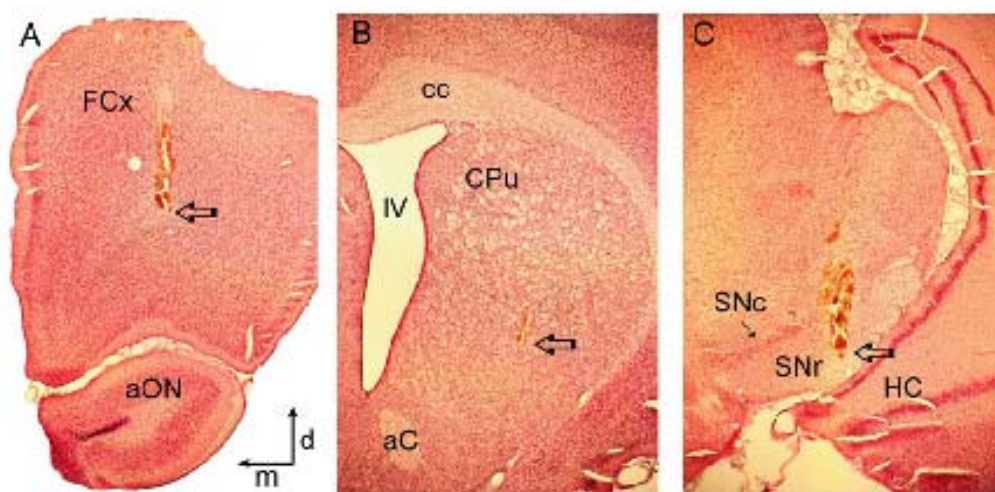


Figure 2.

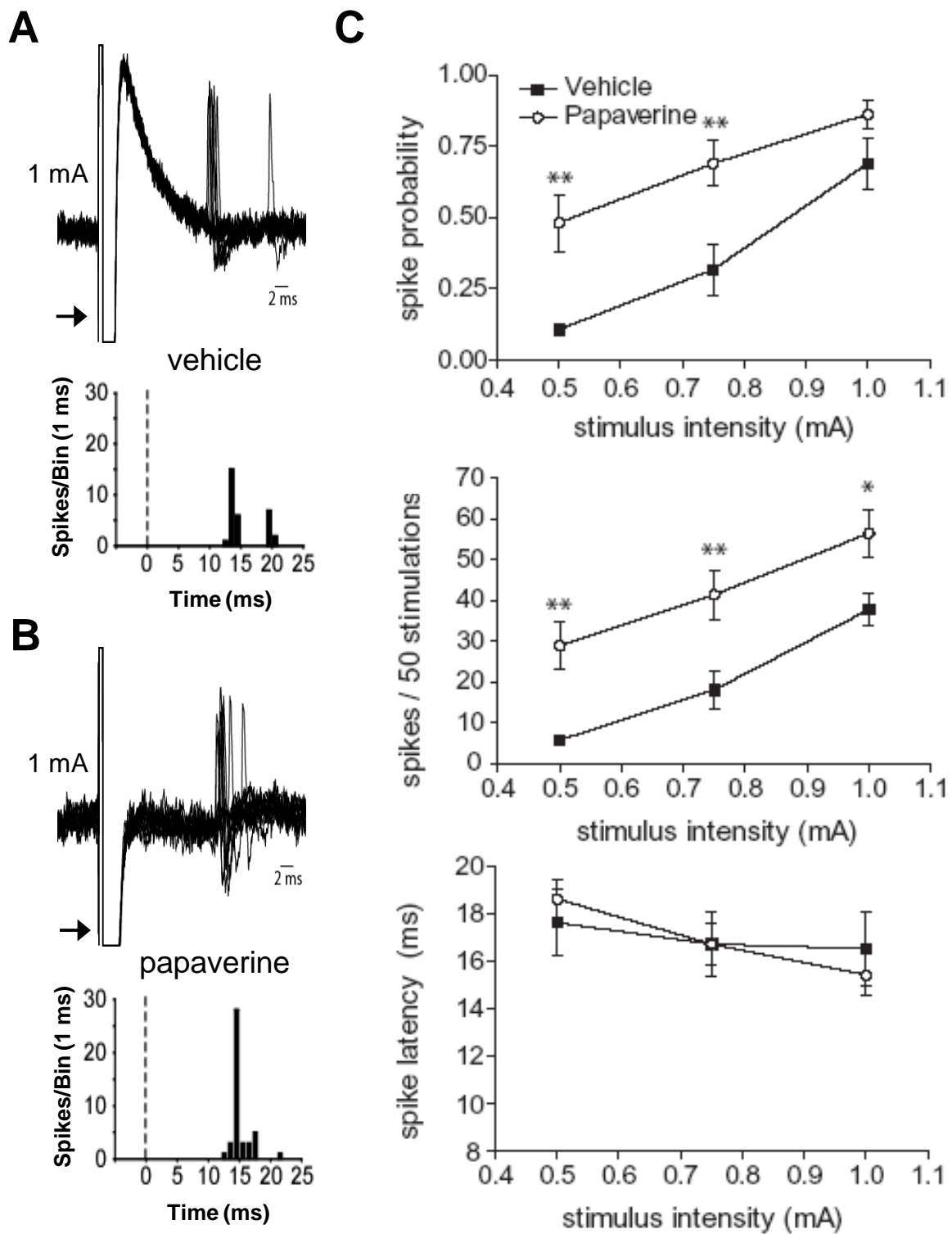


Figure 3.

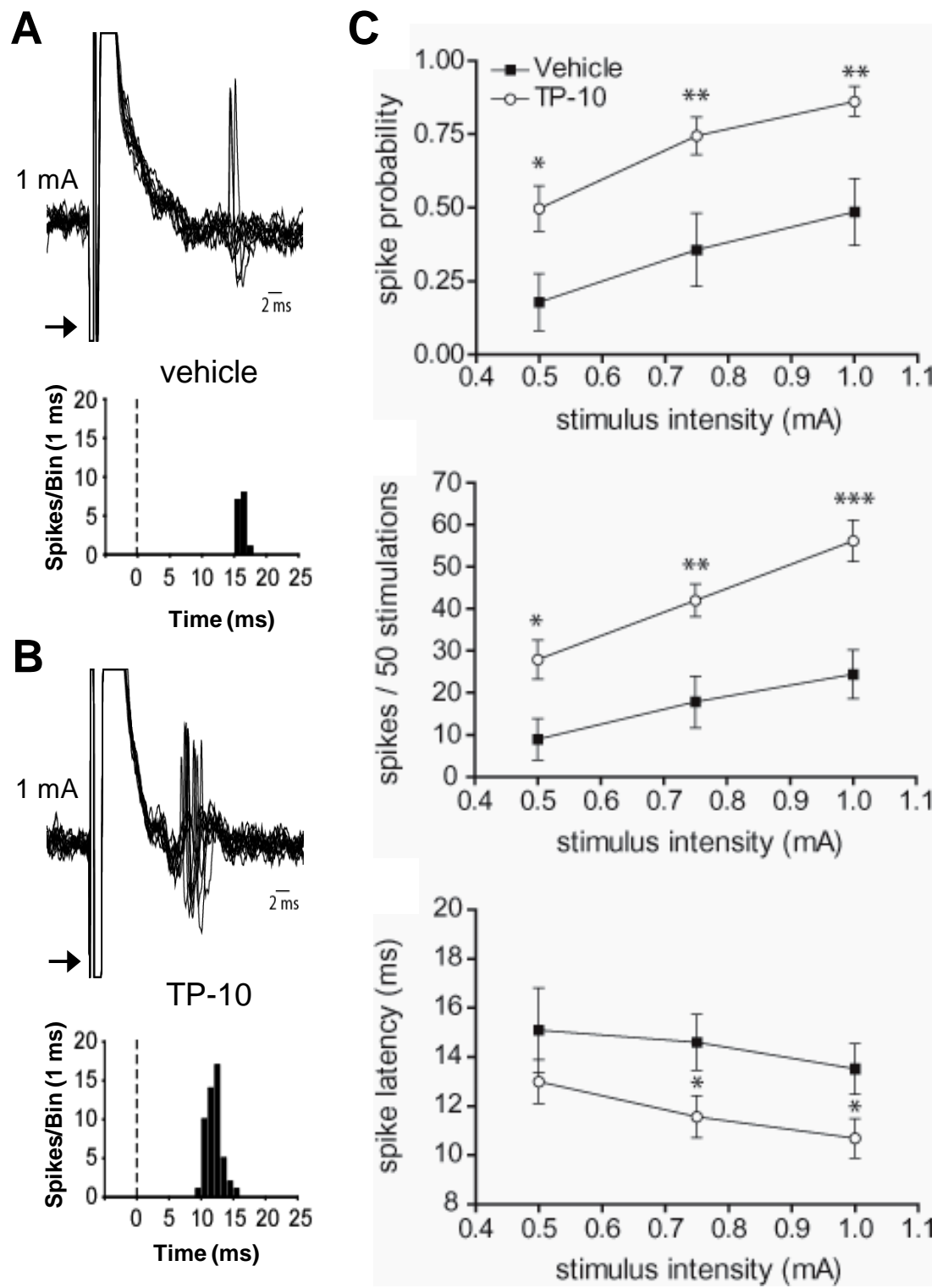


Figure 4.

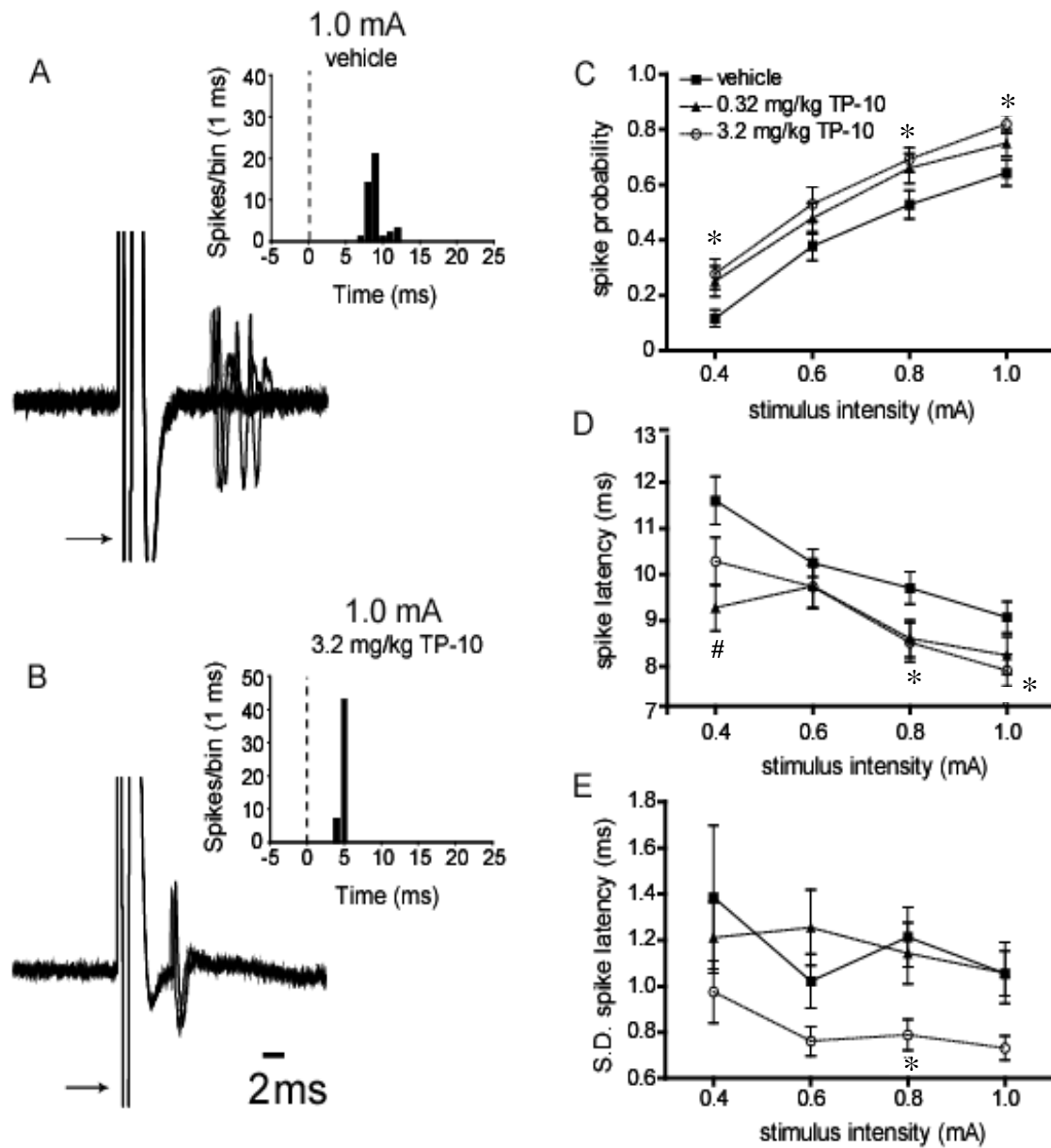


Figure 5.

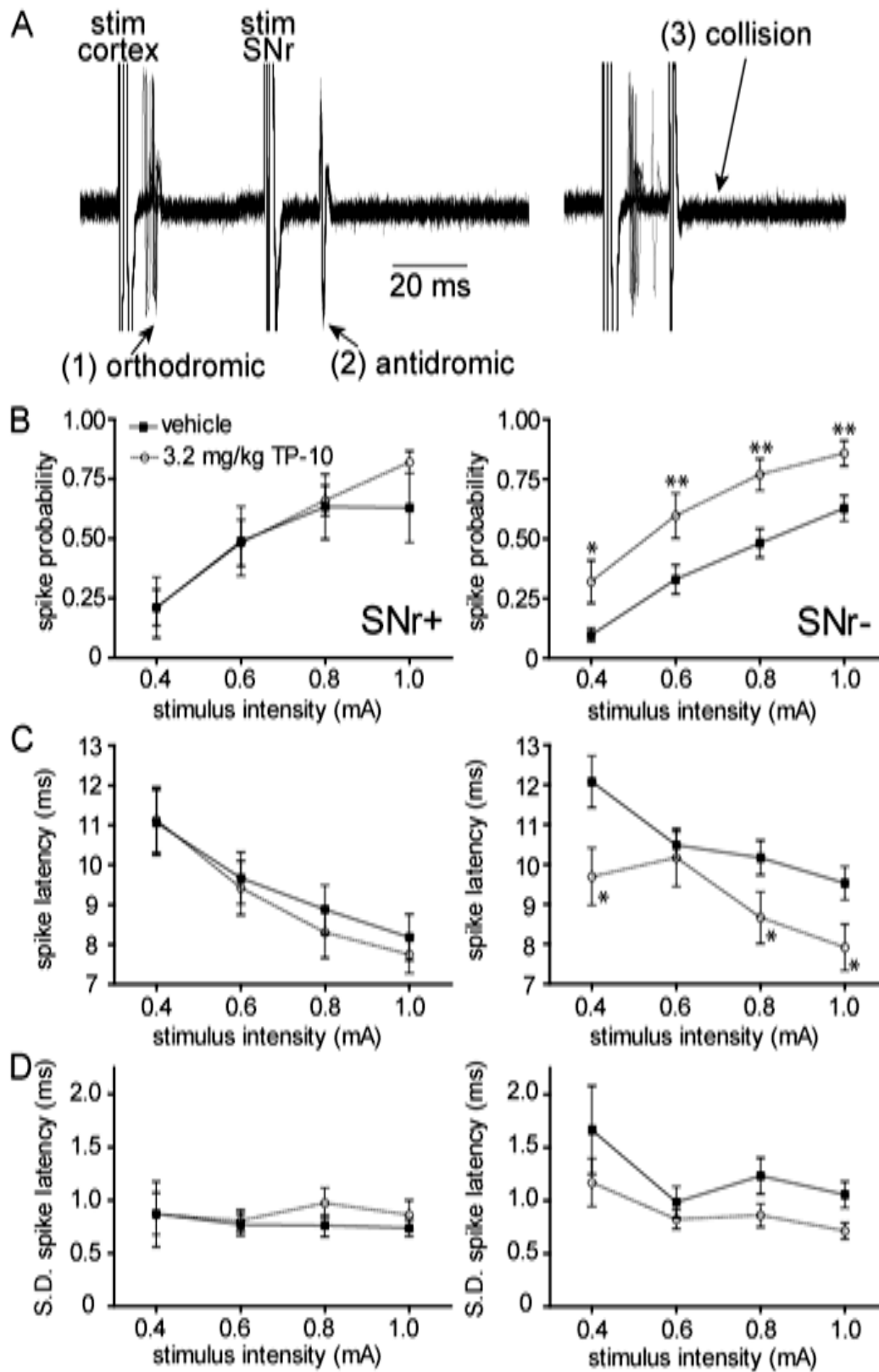


Figure 6.

